STRUCTURE OF THE CONVECTIVE BOUNDARY LAYER DERIVED FROM LARGE-EDDY SIMULATIONS

by Helmut Schmidt and Ulrich Schumann DLR, Oberpfoffen, FRG

Presented at the XXI OSTIV Congress, Wiener-Neustadt, Austria (1989)

ABSTRACT

A large-eddy simulation model is applied to free convection in the atmosphere. Contour plots of instantaneous fields and of conditionally sampled updraft events are presented based on 160 x 160 x 48 grid cells. It turns out that in the case of homogeneous surface heating convection below 0.5 z_i is organized along lines forming a spoke pattern. Under inhomogeneous conditions, this pattern is less pronounced. Isolated updrafts prevail in the upper chimneys by small scale bubbles.

1. INTRODUCTION

Glider pilots as well as sailplane designers, need data on the structure of the convective boundary layer (CBL). Knowledge about the spatial distribution and intensity of vertical motions enables an optimized choice of flight level, cruising speed and circling speed, which is the basis of successful

long distance cross country flights. Engineers promise further improvement of wing profiles as soon as pilots commit themselves to distinct air speeds adapted to the specific conditions of thermal convection.

Since about 1970, rapid sensors on board the aircraft are at the meteorologists' disposal to answer a part of the above questions in terms of spectra of vertical velocity, temperature and humidity along horizontal flight legs (Lenschow and Stephens, 1980, Hafner, 1985). As a result, we have a fairly complete knowledge of the vertical profiles of second- and third-order moments of turbulent fluctuations, horizontal spectra and of probability distributions of vertical velocity and temperature fluctuations at a given height.

During the past few years, two scientific groups have been working on the three-dimensional time-dependent numerical simulation of the CBL, stimulated by the recent development of super computers (Moeng and Wyngaard, 1988, Nieuwstadt and De Valk, 1987 and Mason, 1987). All of them use the technique of large-eddy simulation (LES). This method has reached the status of a third column (besides field and laboratory experiments) in boundary layer research, opening the option of "field programs on the computer" (Wyngaard, 1984).

We report on LES of the CBL over flat terrain with strong thermal convection, due to heating from the surface with weak wind. This type of CBL is referred to as the free convection case. We first present results under the condition of homogeneous surface heating and, afterwards, discuss specific differences caused by spatially variable surface heat flux. In both cases, the air motion exhibits the coherent structure of convective circulations composed of buoyant updraft and compensative down draughts. The CBL is capped by an inversion layer of height z_i with stably stratified air above. As shown by Deardorff (1970), the convective velocity and temperature scales are $w_*=(ßgz_iQ_s)^{1/3}$; $T_*=Q_s/w_*$ and where $ß=1/T$ is the volumetric expansion coefficient and Q_s denotes the surface "temperature flux." The convective timescale $t_*=z_i/w_*$ describes how long a buoyant plume is on its way from the ground to the inversion. For our simulation, we selected values typical for a sunny day in southern Germany: Q_s=0.06 K ms^{-1}, z_i=1600 m, (ß=1/300 K^{-1}) which implies w_*=1.46 ms^{-1}, T_*=0.041K. and t_*=1096s.

2. THE CBL IN TERMS OF VERTICAL PROFILES

Buoyant plumes are by far the most marked structural elements of the CBL. They start at the ground and run through the whole depth of this layer and penetrate into the stable layer aloft. They carry both the highest terminal velocity and maximum temperature deviations. Most of the thermodynamics of atmospheric convection can be attributed to them. Figure 1 relates the temperature excess of an individual thermal to vertical profiles of some well known second moments as vertical heat flux, horizontal and vertical velocity variances and temperature variance.

The computed mean temperature profile shows in the surface layer strongly unstable stratification while between 0.3 z_i and 0.5 z_i the temperature gradient is only weakly negative. At about 0.5 z_i the temperatue gradient changes its sign so that the upper half of the CBL exhibits increasing stability. The position of maximum gradient is near 1.1 z_i.

Relative to the mean profile an individual plume is started at the ground, due to a temperature surplus compared to the mean surroundings of ΔT. While rising ΔT is diminished by turbulent diffusion, which process causes the heating of the whole CBL. Above 0.5z_i the temperature surplus is additionally reduced by the stable mean stratification. At about 0.8z_i, ΔT becomes negative and the updraft is no longer buoyant. Further rising is carried by inertia, due to the high amount of positive vertical momentum gained in the lower mixed layer. The overshooting beyond the level of the inversion causes strongest negative values of ΔT at 1.1 z_i connected with adequate negative buoyancy which stops the movement.

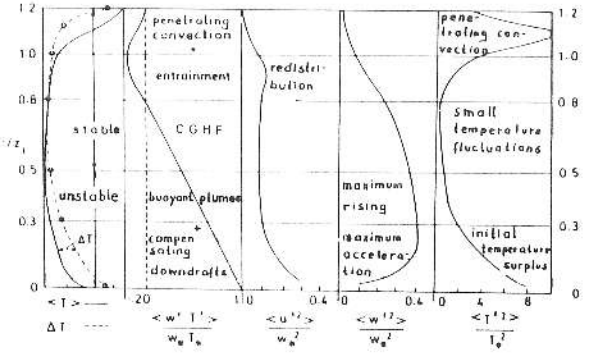

Figure 1. .

The profile of $<T'^2>$ simply can be interpreted as an image of the profile of ΔT. Large variances are observed near the ground and above z_i while the middle portion of the CBL shows only small values of $<T'^2>$. Due to strong buoyancy, plumes are most accelerated near the ground, which is reflected by the increase of $<w'^2>$ from zero at the ground to the maximum value at about 0.4z_i. In the upper layers the vertical velocity variance is decreased gradually by diffusion and above 0.8z_i rapidly by the additional effect negative buoyancy.

Horizontal motions are weaker than updrafts because they are a secondary phenomenon and not directly forced. Nevertheless, the profile of $<u'^2>$ shows an absolute maximum near the surface and a secondary maximum just below z_i. Both maxima reflect a pattern of thermal circulation with centres in the strong updrafts and horizontal redistribution of momentum in the surface and inversion layers.

The positive heat flux in the lower levels is also dominated by buoyant plumes which combine positive temperature fluctuation with positive temperature fluctuation. Between 0.5 z_i and 0.8 z_i heat is transported against the negative gradient of mean temperature, which can easily be understood by the positive ΔT of the strong convective elements. Heat flux changes sign together with ΔT. Negative values of $\langle w'T' \rangle$ above this level are reinforced by warm sinking motions which compensate the penetrative convection and which are referred to as entrainment of air from the stable layer into the mixed layer.

3. THE LARGE-EDDY SIMULATION METHOD

The LES uses a finite-difference method to integrate the three-dimensional grid-volume averaged Navier-Stokes equations. The Overbeck-Boussinesq approximation is used,

i.e. density is assumed to be constant except for buoyance, and temperature T corresponds to the potential temperature in the atmosphere.

Since the dynamics of atmospheric free convection roughly covers a range of six orders of magnitude (few kilometers to few millimeters) only the large (convective) and mesoturbulent scales of motion are resolved by the grid. Microturbulent subgrid-scale (SGS) fluxes are determined from algebraically approximated second-order closure (SOC) transport-equations. All essential coefficients of the SGS-model are determined from the inertial-convective subrange theory of locally isotropic turbulence. The influence of varying SGS-model assumptions and model coefficients on the resolved scale structures are discussed in Schmidt (1988), details of numerical methods are described in Schmidt and Schumann (1989). The computational domain extends horizontally and vertically over a finite domain of size X x X x z, where X = 8000m = $5z_i$ and z = 2400 = $1.5z_i$. The simulation is performed with a computational grid of 160 x 160 x 48 cells, which fully exploits the capacity of a CRAY-XMP computer.

3.1 Boundary Conditions

Since, in this paper, we confine ourselves on the windless (in mean) case and, since the largest convective scales of the order of z_i are contained several times in the computational domain, periodicity is assumed at the lateral boundaries. Convection is driven by the heat flux Q_s which determines the SGS flux at the bottom. The vertical fluxes of horizontal momentum are evaluated from the Monin-Obukhov relationships, which gives us the opportunity to study the influence of varying roughness height z_o on the convection. A radiation boundary condition at the top of the computational domain prevents spurious reflections of gravity waves.

3.2 Initial Conditions

We started our simulation with the following initial conditions: the mixed layer, represented by constant temperature is capped by a layer of uniform stability with a temperature gradient of 3K/1000m. The initial temperature and velocity fields contain random disturbances to initiate the convection with very low amplitudes of $0.1T_*$ and $0.1w_*$ respectively. To reach an asymptotic state a model time of $t/t_*=6$ is expected to be sufficient. Since the convective layer will deepen during this time, we start with z_i = 1350m to end with the planned value of z_i = 1600 = 2z/3 at the time of evaluation.

4. RESULTS

Based on various evaluations, including plots of instantaneous velocity and temperature fields, a computer movie, analyses of two-point correlation functions, conditional mean values and horizontal Fourier spectra, we obtain a rather complete picture of the structure of the CBL.

4.1 Instantaneous Fields

Figure 2 shows contour plots of vertical velocity and of temperature fluctuations in an arbitrary vertical cross-section. The velocity field exhibits some strong and narrow updrafts, which extend over the whole CBL. In the lower levels, it corresponds well to positive values in the temperature field, while near the inversion layer the rising air is cooler than the surrounding in the same level. Both the velocity and the temperature contours show several local

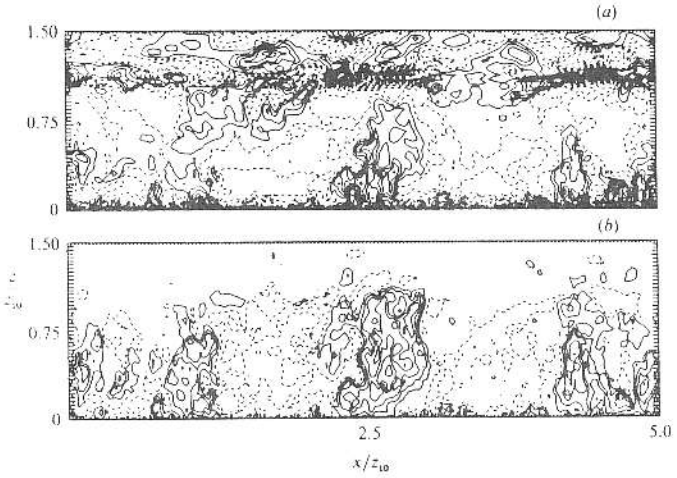

Figure 2.

maxima, which we call bubbles in the updrafts. A computer movie generated from a sequence of such plots shows that a couple of small scale bubbles rise inside quasi steady updrafts in sequence. The bubbles are rising more quickly than the average updraft, their lifetime scales are of order $0.1t_*$.

The rather narrow updrafts are surrounded by large areas of downdrafts which form for continuity. This can be seen in Figure 2 and also in Figure 3, which presents horizontal cross-sections of the same fields at two height levels. The imbalance of updrafts and downdrafts implies a skewed velocity distribution: A pilot will meet sinking air more frequently than rising air, but nowhere is the sinking as strong as the rising in the plume centers. This is also reflected by Figure 4 which shows the area fraction and mean velocities in the updrafts and downdrafts. Note the high and almost constant rising velocities at about $0.25 <= z/z_i <= 0.75$ which implies that this height interval offers the best chance to rise by circling. In the upper third of the CBL the intensity of updrafts decays rapidly (Schumann and Schmidt, 1988).

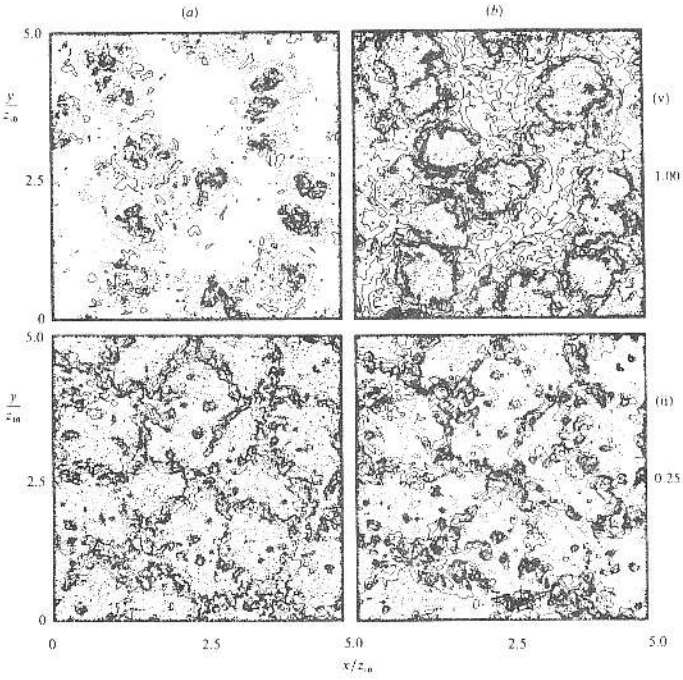

Figure 3.

Another feature of CBL's vertical motion well known to glider pilots is that near the ground (and near the inversion level) small scale motion is dominant. Nevertheless, the surface layer is well organized rather than chaotic: Polygonal spoke-patterns characterize the structure of convection near the surface. The pattern is that of open cells with a sinking motion at the cell's center. The polygonal pattern is induced by wide downdrafts which suppress upward motions over most of the surface and drive the surface flow radially away from the center of downdrafts. The air then converges towards lines and it appears quite natural that these lines form polygonals, due to competing downdrafts (see Figure 5). Due to the convergence and to the temperature surplus gained through the close contact to the heated surface the air rises along the spikes. There are also a few measurements which show that near the surface rising motion is organized rather along narrow spikes than in more or less isolated thermals (Wallington, 1983). That might be a hint to pilots to change their tactic of circling when being unfortunately trapped in heights of less than 0.25 z_i.

Isolated small,scale plumes remote from the main updrafts do not merge together, but die out while rising against downdrafts. The polygonal structure of the surface layer is lost in the middle and upper portion of the CBL. The spikes become divided and the hubs turns out to be the roots of the updrafts and plumes in the upper mixed layer. But, also in this region, the updrafts seldom show the idealized round cross-section. They, instead, are highly convoluted due to strong lateral entrainment.

Entrainment is also an important process at the interface between mixed layer and stable layer: Large thermals formed within the updrafts penetrate into the stable layer and export relatively cool air into the stable layer. They cause large-scale downward movements of wisps of extruded warm air. Both the large upward penetrating thermals and the downward moving wisps contribute to the entrainment heat flux.

In the stable layer, penetrating convection excites a faint gravity wave regime. The amplitudes of the corresponding vertical motions are inside the isoline increment of the w-plot. Nevertheless, high-amplitude large-scale temperature fluctuations accumulate due to the strongly stable stratification, for which the thermal dissipation rate is small. Gravity waves on top of the CBL (often referred to as thermal waves) which are strong enough to carry a sailplane, need different conditions: They have been observed in the presence of a

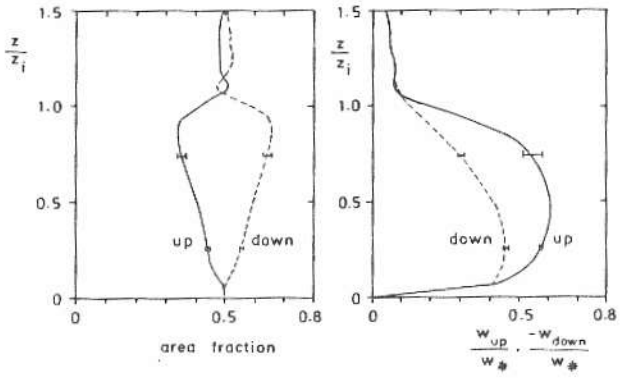

Figure 4. Mean area fraction of updrafts (full curve)and downdrafts (dashed) and mean vertical velocities within these areas. The error bars indicate the scatter of the results within $6 \leq t w_* / z_i \leq 8$ (Schumann and Schmidt, 1989).

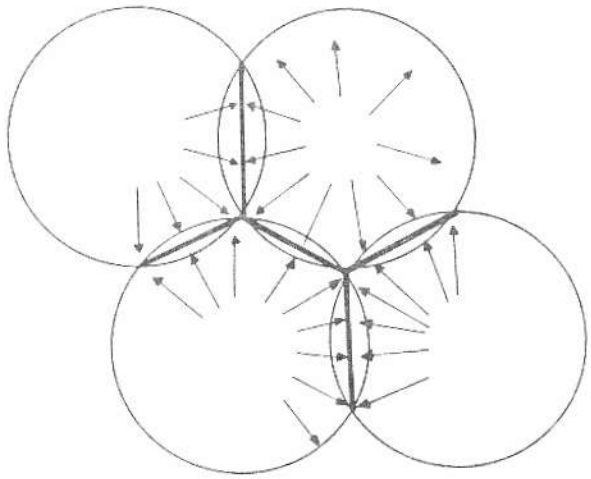

Figure 5. Organization of polygonal spikes at the rim of competing downdrafts in the surface layer.

minimum mean flow accompanied by a shear zone near the inversion layer (Clark and Hauf, 1989).

4.2 Inhomogeneous Surface Heating

We also studied the effect of spatial variations of the surface heat flux as is typical for most of the natural topographies. In this numerical experiment $Q_{s,l}$ in the western part of the domain is half of the heat flux in the eastern part while the mean value of Q_s equals the heat flux in the homogeneous case (see Figure 6). All the other physical and geometrical parameters remain unaffected compared to the last section.

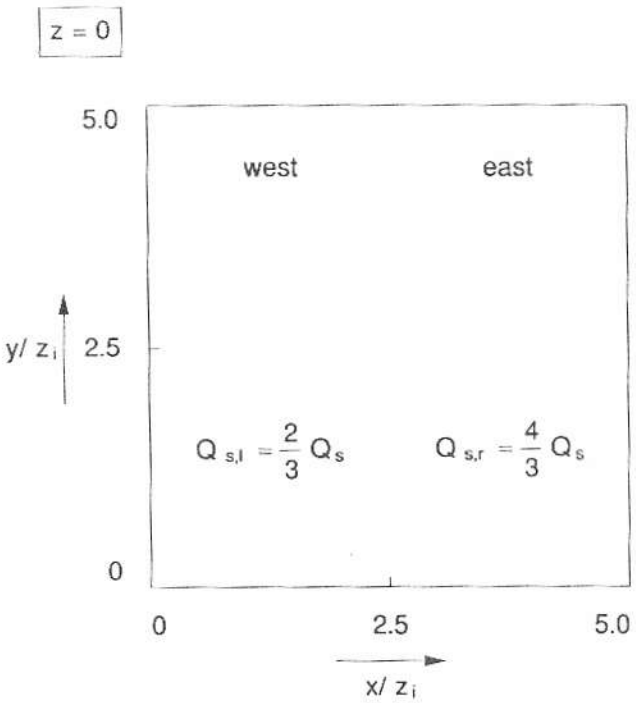

Figure 6.

The flow pattern in the case of differential heating exhibits some specific properties as reflected by some contour plots. Figure 7 shows how in a (x, z)-plane vertical motions build up. Roughly spoken, one role is established with rising motion over the eastern half of the domain and sinking motion over the less heated western part. This large scale pattern is superposed by small scale thermals also over the weakly heated areas. Large heat fluxes not only cause more intense vertical motions, but also list the inversion to a higher level compared to areas of smaller $Q_{s,i}$.

The spoke pattern observed in the lower altitudes of the homogeneously heated CBL is now modified: At the level of $0.125z_i$ (Figure 8a) the air is rising with varying speed along the center line of the strong heat flux area. On the opposite side, the general motion is sinking interspersed with spotlike plumes. Convection organized in spokes or along lines prevails in the intermediate region. Since the inversion is a sloped plane (Figure 8 refers to the average inversion height) z_i is obviously cut by the cross section of the lower plot in Figure 8b: While the left western part of the domain shows only very weak (positive) vertical motions typical for the stable layer the stronger heated eastern part in the same level exhibits strong upward motion along a line only partially turned into isolated thermals.

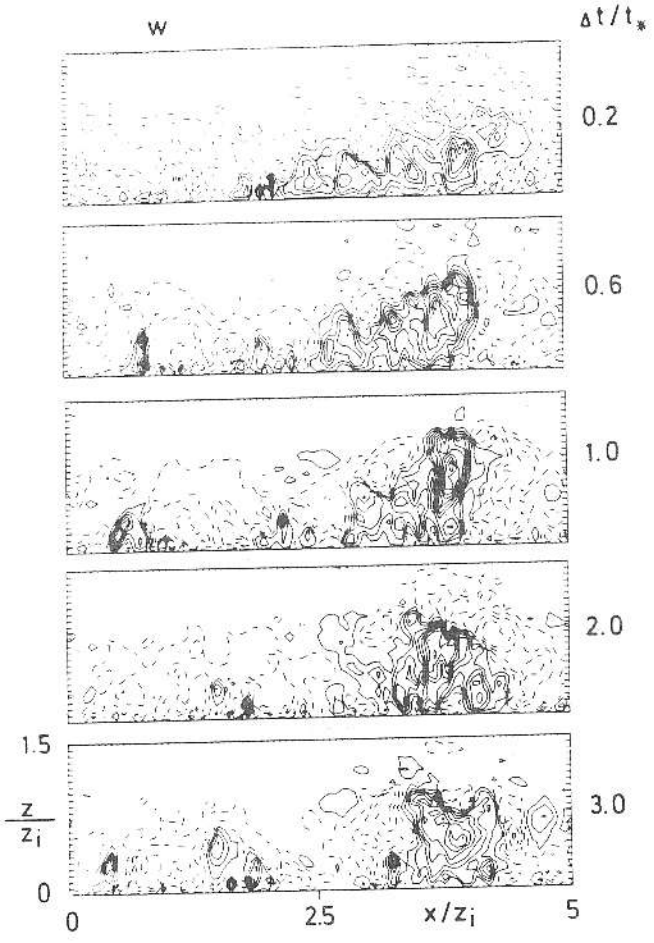

Figure 7. Inhomogeneous heating: Contour plots of vertical velocity w/w_* for x/z_i versus z/z_i at different times t/t_* after initialization in a vertical plane. Countour line increments correspond to those in Figure 2.

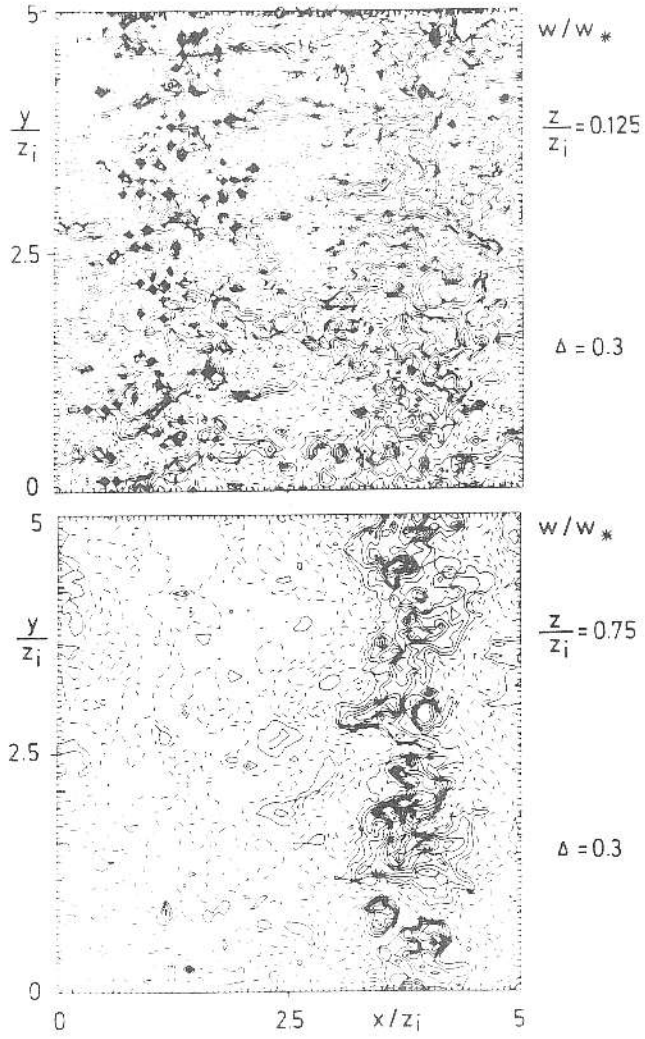

Figure 8.

4.3 Conditionally Averaged Updrafts

The contour plots of Figures 2 and 3 show the instantaneous shape of few updrafts. The three-dimensional LES data of the homogeneous run allow for the evaluation of the mean spatial structure of the CBL. To achieve this, we have conditionally sampled events of updrafts (and downdrafts), using vertical velocity as an indicator function. Details of this sampling method are described in Schmidt and Schumann (1989). Figure 9 depicts six contour plots in a vertical plane through the axis of symmetry related to positive w-events with a threshold equal to the r.m.s. velocity at the reference level $z_c=z_i/2$. The results represent mean values over 400 time steps from $t/t_* = 6$ to 7. If we assume that the lifetime of small-scale thermals is of order $0.1t_*$ then we average over approximately 160 independent events.

The conditionally averaged updrafts have large vertical velocity (maximum value = $2.0w_*$). The horizontal radius is approximately $0.33z_i$. Rising is correlated with horizontal velocities which show maxima in the surface layer (inflow) and just below z_i (outflow). A secondary maximum of u just above the reference level also indicates motion away from

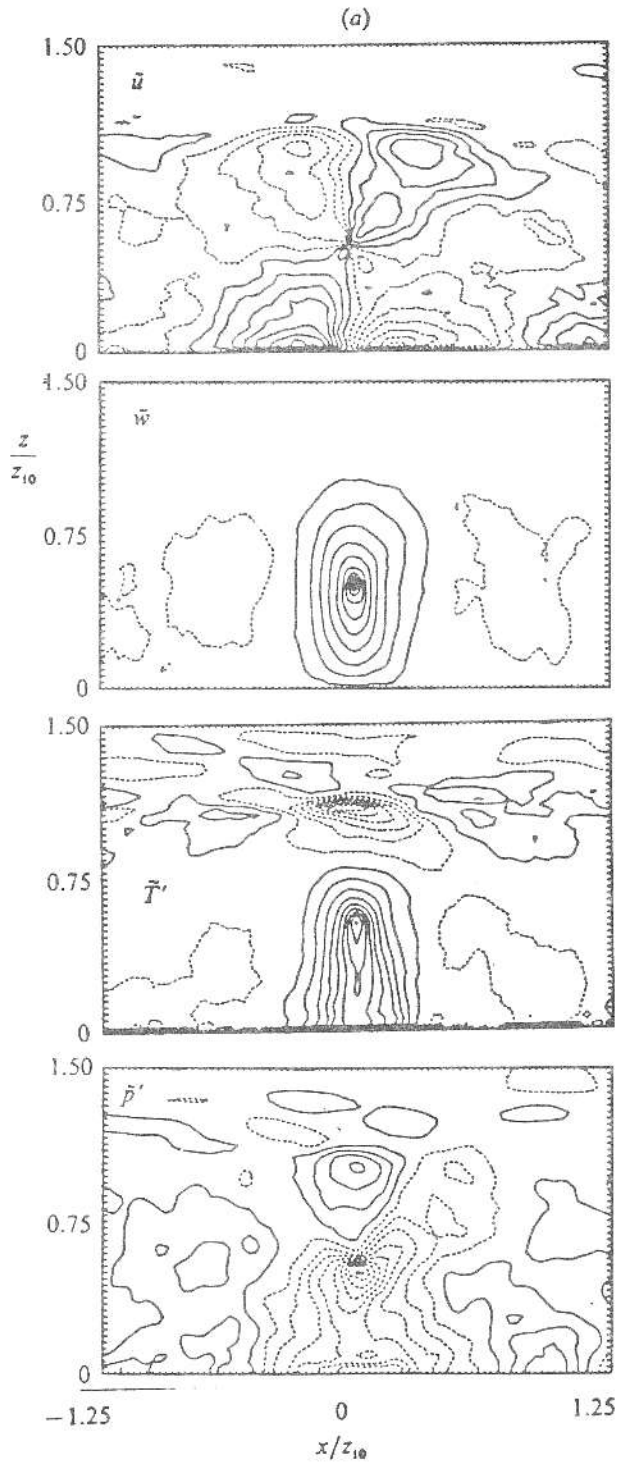

Figure 9.

the updrafts and is due to bubbles in the updrafts, which displace air sideway while rising.

The temperature pattern also shows a coherent structure which extends from the surface up to the inversion. The maximum temperature surplus amounts to 2.7T, in the reference level. In contradiction to the T-field, vertical velocity values are quite small near the surface. Most of this difference can be explained by the different conditions for a buoyant plume to start from the surface. Initially, it has maximum temperature surplus but zero vertical velocity. The updrafts cause negative temperature fluctuations in the interfacial layer, where most of the temperature surplus has been dissipated and the stratification becomes more and more positive. The upward motion above this level is driven by inertia while slowed down by negative buoyancy.

The pressure signal is obviously most affected by the large-scale dynamics of the updrafts and the pressure fluctuation is negative below the thermal. This behavior is to be expected from hydrostatic considerations, but is also caused by buoyant bubbles which suck in air from below and from the sides. Pressure fluctuations assume a positive maximum near the inversion, presumably because of a pressure head, due to thermals impinging on the inversion.

5. REFERENCES

Clark, T.L. and T. Hauf, 1989: Three-dimensional Numerical Experiments on Convectively Forced Internal Gravity Waves. *Q.J.R. Meteorol. Soc., 115*, 309-333.

Deardorff, J.W., 1970: Convective Velocity and Temperature Scales for the Unstable Planetary Boundary Layer and for Rayleigh Convection. *J. Atmos. Sci., 27*, 1211-1213.

Hafner, T., 1985: Structure and Horizontal Distribution of Thermal Updrafts in a Cloudless Boundary Layer in South-Bavaria. *OSTIV Publication XVIII.*

Lenschow, D.H. and P.L. Stephens, 1980: The Role of Thermals in the Convective Boundary Layer. *Boundary-Layer Met., 19*, 509-532.

Moeng, C.H. and J.C. Wyngaard, 1989: Recent Large-Eddy-Simulation Results for the Convective Boundary Layer. *J. Atmos. Sci.*

Mason, P.J., 1989: Large-Eddy-Simulation of a Convective Atmospheric Boundary Layer. *J. Atmos. Sci.*

Nieuwstadt, F.T.M. and J.P.J.M.M. de Valk, 1987: A Large-Eddy-Simulation of Buoyant and Non-buoyant Plume Dispersion in the Atmospheric Boundary Layer. *Atmos. Environ. 21*, 2573-2587.

Schmidt, H., 1988: Grobstruktur-Simulation konvektiver Grenzschichten. *DFVLR-FB 88-30.*

Schmidt, H. and U. Schumann, 1989: Coherent Structure of the Convective Boundary Layer Derived from Large-Eddy Simulations. *J. Fluid Mech. (1989)*, 200-511-562.

Schumann, U. and H. Schmidt, 1989: Heat Transfer by Thermals in the Convective Boundary Layer. *H.H. Fernholz and H.E. Fiedler (Eds.): Proceedings of the 2nd European Turbulence Conference*, Berlin 1988, Springer-V, Heidelberg (1989).

Wallington, C.E., 1983: Potential Exploration and use of Miniscale Lift Patterns. *OSTIV Publication XVIII.*

Wyngaard, C.C., 1984: Large-Eddy-Simulation. *Guidelines for its Application to Planetary Boundary Research.* DTIC 84 09 28 033.